V. KRIVENYUK, I. MAMUZIĆ

ISSN 0543-5846
METABK 46 (2) 79-85 (2007)
UDC - UDK 539.4:621.762=111

CORRELATION OF CREEP-RUPTURE DATA FOR COMPLEX ALLOYS AT ELEVATED TEMPERATURES

Received - Primljeno: 2005-11-05
Accepted - Prihvaćeno: 2006-08-20
Original Scientific Paper - Izvorni znanstveni rad

The main tendency towards the development of the methods for predicting long-time data on of metallic materials is to derive the correlation relationships, which should be as general as possible. This paper presents the verification of the fact that a sufficiently accurate estimation of the peculiarities of the portions of experimental diagrams and generalization of this information can be of great importance for a considerable progress in the prediction.

Key words: *creep, Cr-Mo-V alloys, prediction, interpolation, time, temperature*

Korelacija karakteristika puzanja složenih legura. Glavna tendencija u razvitku metoda prognoziranja puzanja metalnih materijala sastoji se u dobivanju korelacijskih odnosa, koje bi bile po mogućnosti što jednostavnije. Članak je posvećen pojašnjenju za dovoljno točno određivanje svojstava pojedinih dijelova eksperimentalnog dijagrama, a ove informacije imaju veliki značaj za vrednovanje napredovanja u prognoziranju.

Ključne riječi: *puzanje, Cr-Mo-V legure, prognoziranje, interpolacija, vrijeme, temperatura*

INTRODUCTION

Among the parametric approaches to the prediction of the stress-rupture data for metals, the best known are the Larson-Miller (LM), Manson-Haferd (MH), Orr-Sherby-Dorn (OSD) [1-3] parameters

$$P_{LM} = f(\sigma) = T(C + \lg t), \tag{1}$$

$$P_{MH} = f(\sigma) = \frac{\lg t - \lg t_a}{T - T_a}, \tag{2}$$

$$P_{OSD} = f(\sigma) = \lg t - \frac{B}{T}, \tag{3}$$

$$f(\sigma) = b_0 + b_1 \lg\sigma + b_2 \lg^2\sigma + ... + b_n \lg^n\sigma, \tag{4}$$

where:

t - the time to rupture /h,
T - temperature /K,
C, t_a, T_a, B - optimized parametric constants, and
b_0, b_1, b_2,…, b_k - the regression coefficients.

V. Krivenyuk, G. S. Pisarenko Institute for Problems of Strength National Academy of Sciences of Ukraine, Kiev, Ukraine, I. Mamuzić, Faculty of Metallurgy University of Zagreb, Sisak, Croatia

A distinguishing feature of the parametric methods consists in merging of several stress-rupture (SR) curves into a single curve. The deviations from the established correlation relations are encountered frequently, and they are, in fact, ignored. Moreover, simulation of the process of weakening is performed with a large number of essential simplifications. For instance, various models have been experimentally justified for certain limited conditions, but in reality those limitations are not taken into account. As a result, these correlations have been accepted by some and roundly criticized by others.

The LM method is physically justified. Thereupon, it is expedient to consider in more detail the constant C, to which the physical meaning is attached in many researches. To determine the constant C, we use the following formula [4]:

$$C = \frac{T}{\Delta T} m' \log\frac{\sigma_1}{\sigma_2}, \tag{5}$$

where σ_1 and σ_2 are the creep rupture strength values at $t = const$ found, for example, from two rectilinear SR curves at T_1 and $T_2 = T_1 + \Delta T$ and m' is the cotangent of the SR curve slope at the temperature T_1.

Formula (5) has been obtained as a result of transformation of expression (1). From (5) it follows that in the

case where C is estimated on the basis of the data for two rectilinear SR curves at the temperatures T_1 and $T_2 = T_1 + \Delta T$, the value of C depends on the mutual position of the curves. If the curves are parallel, $C = const$. If their slope changes essentially from one curve to another, then, as the time to rupture increases, the logarithm of the quotient in (5) increases and leads to a significant dependence of the characteristic C on time. Hence, for equidistantly located curves, the time dependence of the constant C is weak, while for the curves that are distinguished by the slopes, it may be sharp.

In investigations of refractory metals, calculations often give rather low values of the constant C. Thus, as a result of processing the stress rupture data for tungsten [5], C = 12,2 was obtained and for Ta-10W alloy C = 10,8. Similarly, for molybdenum it was found that C = 13,5. This differs significantly from the quantity 20 that is commonly used for many materials. Within the framework of the traditional investigations, this leads to the conclusion that the constant C is sensitive to the material class. Actually, in the case under consideration, the difference in the constant C values for refractory and heat-resistant steels and alloys is mainly determined by a considerable time dependence of this constant. The point is that refractory metals are primarily studied at short loading times, whereas heat-resistant materials at long times, which results in higher values of C for heat-resistant steels and alloys according to formula (5).

The SR curves considered in Figure 1. are to some extent representative for the maximum wide temperature range of creep rupture tests as a whole. At the minimum

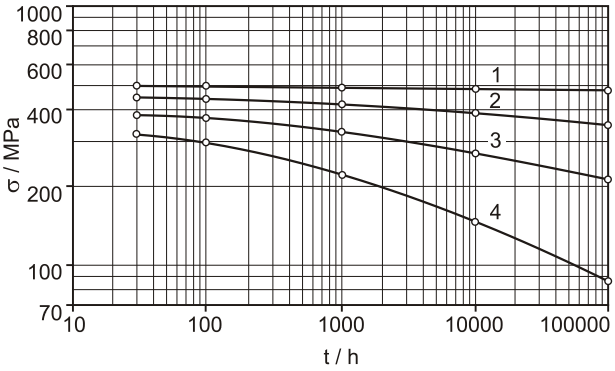

Figure 1. **Cr-Mo-V creep rupture data [6] at 400 (1), 450 (2), 500 (3), 550 °C (4)**
Slika 1. **Puzanje legure Cr-Mo-V [6] pri 400 (1), 450 (2), 500 (3) i 550 °C (4)**

temperatures, the slope of SR curves is often close to the horizontal one, and at the maximum temperatures, creep-rupture strength decreases to low values (10-30 MPa) and lower. In these cases, the difficulties are encountered that were noted in part by the authors of [6] and which may be judged by the transition from the SR curves in Figure 1. to the parametric curves in Figure 2.

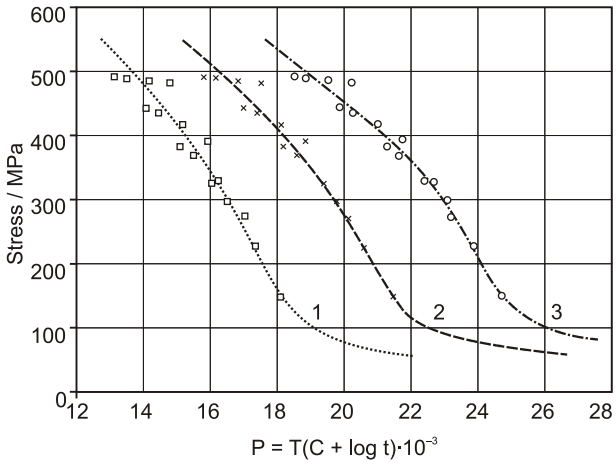

Figure 2. **Results of the Larson-Miller method data processing [6] (Figure 1.) at the values of C and S_1 equal to 18 and 1,32 (1); 22 and 1,36 (2); 26 and 1,46 (3)**
Slika 2. **Rezultati obrade Larson-Miller-ovom metodom prikazani na slici 1. pri vrijednostima C i S_1 jednakim 18 i 1,32 (1); 22 i 1,36 (2); 26 i 1,46 (3)**

As a preliminary, it should be emphasized that parametric transformations for obtaining parametric curves practically do not change the slopes of individual SR curves with respect to each other at different temperatures. Therefore, as follows from Figure 2., at the minimum temperature the SR curve sharply deviates from the parametric curve, which, in general, is a source of significant errors, while at the maximum temperatures, the cause of possible significant errors can be as follows.

At medium temperatures, as can be judged from curves 2 and 3 in Figure 1. and from their mappings in Figure 2., when obtaining a parametric curve for curve 2 with increasing temperature and decreasing stress, curve 3 is an important refining reference curve. For the curve at the maximum temperature, in this case this is curve 4, there is no such refining reference curve. As a result, the effect of the experimental data scatter on the shape of the estimated parametric curve may rise sharply. This can be judged from the following example.

Based on the data in Figure 1., parametric curves were obtained as shown in Figure 2. In this case, after the interpolation calculations, a prediction was made at a rather high value of S_1: S_1 = 1,32 and C = 18. At the values of C equal to 22 and 26, the S_1 values turned out to be equal to 1,36 and 1,46. The parametric curves were also calculated by varying only the time at a temperature of 550 °C and σ_t = 226,3 MPa which were chosen arbitrarily as an example. In the former case, 2000 h were taken as the time to rupture instead of 1000 h. At the C values equal to 18, 22, and 26, such change in the time to rupture resulted in lower values of S_1 equal to 1,28, 1,15 and 1,10. In the latter case, 500 h were accepted instead of 1000 h. At the C values equal to 18, 22 and 26, the value of S_1 increased sharply to 1,79, 1,93 and 2,11.

MATERIALS, TREATMENT, AND TESTING

A distinguishing feature of the base diagram method [4, 7, 8] is the manipulation of deviations of individual portions of the experimental or calculated diagrams from the corresponding portions of the base diagrams. Base diagrams are described by the following general equation with specified constants:

$$\lg \sigma_t' = \lg \sigma_1 - \frac{3,6 - \lg \sigma_1}{12}\left(\lg t + 0,1 \cdot \lg^2 t\right), \quad (6)$$

where:

σ_t' - the current stress value from the base diagram / MPa,
σ_1 - the one-hour strength /MPa, and
t - the time to rupture /h.

Table 1. **Results of processing data [13] for heat 20G by BDM**
Tablica 1. **Rezultati obrade podataka [13] za talinu 20G s BD metodom osnovnih dijagrama**

No.	T / °C	$\sigma_{\alpha t}$ / MPa	σ_{te} / MPa	αt / h	te / h	$\lg(\frac{te}{\alpha t})$	β_3	β_i	Δ_1	Δ_2
1	450	412,0	392,0	0,5	68,2	2,135	0,10	0,13	0,20	– 0,005
2	450	412,0	373,0	0,5	3835,4	3,885	0,10	0,15	0,38	0,007
3	450	392,0	373,0	68,2	3835,4	1,750	0,10	0,14	0,06	– 0,002
4	450	373,0	294,0	3835,4	48420,7	1,101	0,70	0,86	0,20	0,038
5	450	373,0	265,0	3835,4	93425,4	1,387	0,70	0,96	0,48	0,092
6	500	333,0	294,0	116,9	1030,3	0,945	0,70	0,54	0,27	– 0,049
7	500	333,0	265,0	116,9	2783,7	1,377	0,70	0,67	0,15	– 0,028
8	500	333,0	265,0	116,9	7790,7	1,824	0,70	0,52	0,60	– 0,108
9	500	333,0	235,0	116,9	5533,9	1,675	0,70	0,81	0,18	0,035
10	500	294,0	196,0	1030,3	13886,5	1,130	1,30	1,23	0,11	– 0,046
11	500	294,0	157,0	1030,3	35646,2	1,539	1,30	1,30	0,05	– 0,025
12	500	294,0	137,0	1030,3	52982,6	1,711	1,30	1,36	0,04	0,020
13	500	265,0	157,0	2783,7	35646,2	1,107	1,30	1,47	0,13	0,061
14	500	265,0	137,0	2783,7	52982,6	1,280	1,30	1,53	0,22	0,117
15	550	294,0	196,0	77,8	496,2	0,805	1,30	1,73	0,25	0,112
16	550	294,0	157,0	77,8	1448,6	1,270	1,30	1,58	0,26	0,132
17	550	294,0	118,0	7,8	4006,2	1,712	1,30	1,56	0,34	0,209
18	550	294,0	88,0	77,8	11854,2	2,183	1,30	1,49	0,31	0,231
19	550	294,0	69,0	77,8	35165,5	2,655	1,30	1,39	0,14	0,122
20	550	294,0	69,0	77,8	45351,5	2,766	1,30	1,35	0,03	0,024
21	550	294,0	53,0	77,8	145440,1	3,272	1,30	1,28	0,21	– 0,207
22	550	157,0	69,0	1448,6	35165,5	1,385	1,30	1,45	0,14	0,093
23	550	157,0	69,0	1448,6	45351,5	1,496	1,30	1,36	0,03	0,015
24	550	157,0	53,0	1448,6	145440,1	2,002	1,30	1,27	0,13	– 0,101
25	550	118,0	69,0	4006,2	35165,5	0,943	1,30	1,38	0,04	0,023
26	550	118,0	69,0	4006,2	45351,5	1,054	1,30	1,26	0,08	– 0,046
27	550	118,0	53,0	4006,2	145440,1	1,560	1,30	1,21	0,20	– 0,135
28	550	88,0	53,0	11854,2	145440,1	1,089	1,30	1,10	0,23	– 0,146
29	600	157,0	88,0	27,3	473,5	1,239	1,30	1,30	0,05	– 0,027
30	600	157,0	69,0	27,3	1378,6	1,703	1,30	1,26	0,13	– 0,081
31	600	157,0	53,0	27,3	3675,4	2,129	1,30	1,25	0,19	– 0,145
32	600	88,0	53,0	473,5	3675,4	0,890	1,30	1,32	0,02	– 0,009
S_1 = 0,229; S_2 = 0,102; β_1 = 1,3; β_2 = 0,7; β_3 = 0,1; σ_α = 300 MPa; σ_β = 380 MPa										

The left-hand endpoint of an individual portion of the experimental curve in stress and time is denoted as $\sigma_{\alpha t}$ and αt, respectively, and the right-hand one as σ_{te} and te, respectively, for the relation $te/\alpha t \approx 10$.

Using Eq. (6), specific features of each individual segment are characterized by the quantity

$$\beta_e = \frac{\sigma_{\alpha t} - \sigma_{te}}{\sigma_{\alpha t} - \sigma_t'} = \frac{\Delta\sigma_{te}}{\Delta\sigma_t'}, \tag{7}$$

which is an experimentally obtained characteristic of deviation of the portion of the experimental curve in the range between αt and te from the corresponding portion of the base diagram in the range between αt and t at $te = t$. For example, to determine β_e from Eq. (7) at $\sigma_{\alpha t} = \sigma_{100} = 400$ and $\sigma_{te} = \sigma_{100} = 340$ MPa, the values of $\sigma_{\alpha t} = 400$ MPa and $\alpha t = 100$ h are first substituted for σ_t' and t in Eq. (6) resulting in the equation with one unknown σ_1. The obtained value of σ_1 defines the base diagram that passes through the point with the initial coordinates $\sigma_{\alpha t}$ and αt. Next, by substituting the established σ_1 into Eq. (6), we can calculate σ_t' for $t = te$ and determine the quantity β_e from Eq. (7).

After substitution of σ_t for σ_{te} and β for β_e, Eq. (7) is used in the form

$$\sigma_t = \sigma_{\alpha t} - \beta\left(\sigma_{\alpha t} - \sigma_t'\right) \tag{8}$$

to predict the sought value of σ_t from the initial value of $\sigma_{\alpha t}$ using β, which is a generalized coefficient of deviations of individual portions of the experimental curves from the corresponding portion s of the base diagrams. The prediction errors are calculated from the formulas

$$\Delta_1 = \lg t - \lg te, \tag{9}$$

$$\Delta_2 = \frac{\sigma_t - \sigma_{te}}{\sigma_{te}}, \tag{10}$$

and S_1 and S_2 are calculated by substituting the Δ_1 values at $m = 1$ or the Δ_2 values at $m = 2$, respectively, into the following equation:

$$S_m = \sqrt{\frac{1}{n-1}\sum_{i=1}^{n}\left(\Delta_m\right)_i^2}. \tag{11}$$

Equations (6) and (7) allow representing the information on an individual portion of the experimental SR curve as a point (β_e, $\sigma_{\alpha t}$) in the system of β_e, $\sigma_{\alpha t}$ coordinates (Figure 3., Tables 1., 2.). This makes it possible to analyze large data arrays in a simple and efficient manner and provides favourable conditions for the transition to the systematic analysis of the known experimental data. The important constituents of such analysis are the estimation and accounting of the β, β_e, Δ_1, Δ_2, S_1 and S_2 characteristics for different groups of materials.

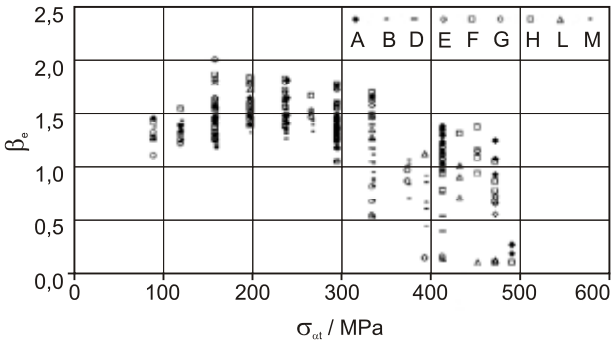

Figure 3. **Experimental creep-rupture data for nine 0,5Cr-0,5Mo steel heats [13] in the β_e - σ_t coordinates (here: A - M the number of the heat)**

Slika 3. **Eksperimentalni podaci puzanja za devet talina čelika 0,5Cr-0,5Mo [13] u koordinatama β_e - σ_t (ovdje je A - M broj talina)**

For solution hardened alloys, the most probable values in the temperature range of practical importance are $\beta = 1\ldots1{,}3$, whereas for precipitation-hardened alloys $\beta = 1{,}4\ldots1{,}7$. The above ranges of β values are mainly explained by an increase in the experimental β_e values as the time of loading and temperature rise. The investigations performed lead to the conclusion that β_e generally varies between 0 and 2,2…2,3 and takes its minimum values, i.e., $\beta_e \approx 0$, when the softening processes almost do not reveal themselves with time and SR curves are nearly horizontal. Such cases are rare. Within a very small range of low temperatures the values of β_e increase rather

Table 2. **Results of processing data [13] by MH and BDM-2**

Tablica 2. **Rezultati obrade podataka [13] metodama Menson-Haferda (MH) i osnovnih dijagrama (BDM-2)**

MH			BDM-2							
Heats	n	S_1	n	β_1	β_2	β_3	σ_α/MPa	σ_β/MPa	S_2	S_1
AH*	234	0,473	283	1,40	1,10	0,30	340	480	0,156	0,459
A	27	0,348	34	1,37	1,10	0,23	420	480	0,121	0,225
B	25	0,447	34	1,40	1,00	0,11	300	400	0,110	0,208
D	22	0,157	20	1,40	0,64	0,70	340	460	0,086	0,167
E	26	0,113	32	1,55	1,20	0,70	340	460	0,125	0,154
F	27	0,426	34	1,42	1,04	0,14	340	480	0,143	0,260
G	27	0,378	32	1,34	0,74	0,14	300	380	0,102	0,229
H	27	0,380	37	1,48	1,07	0,10	340	460	0,112	0,182
L	29	0,393	31	1,43	1,00	0,11	340	440	0,106	0,177
M	24	0,242	29	1,32	0,80	0,53	300	380	0,080	0,191

*AH – All heats

Table 3. **Results of processing data [9 - 14] by the parametric methods for conditions 7, 23, 41, 5, 20, 13**
Tablica 3. **Rezultati obrade podataka [9 - 14] parametrijskim metodama za stanja 7, 23, 41, 5, 20, 13**

Heat	Method	n	S_1	C	Q. / kJ/mol	T_a	log t_a	b_0	b_1	b_2	b_3	b_4	b_5
AH7*	LM	207	0,414	15,7				$1{,}23\cdot10^5$					
7G	LM	18	0,074	24,2				$41{,}1\cdot10^5$	$-1{,}47\cdot10^5$	$0{,}68\cdot10^5$	$-0{,}107\cdot10^5$		
7M	LM	25	0,118	18,6				$7{,}5\cdot10^5$	$-95\cdot10^5$	$888\cdot10^5$	$-41{,}2\cdot10^5$		
AH23	LM	29	0,023	18,6				$-1{,}5\cdot10^5$	$15{,}0\cdot10^5$	$-10{,}8\cdot10^5$	$3{,}44\cdot10^5$	$-0{,}4\cdot10^5$	
23A	LM	86	0,162	18,5				$2{,}95\cdot10^3$	$3{,}4\cdot10^5$	$-2{,}4\cdot10^5$	$0{,}75\cdot10^5$	$-0{,}08\cdot10^5$	
41B	LM	24	0,416	8,94				$33{,}6\cdot10^3$	$39{,}1\cdot10^3$	$-20{,}5\cdot10^3$	$3\cdot10^3$		
AH5	MH	312	0,283			360	14,1	0,7	$-30{,}6\cdot10^3$	$15{,}4\cdot10^3$	$-2{,}85\cdot10^3$		
5B	MH	26	0,092			230	19,5	– 0,02	– 2,0	2,26	– 1,24	0,33	– 0,03
5M	MH	77	0,091			420	13,4	13.4	– 0,01	– 0,005			
AH20	MH	234	0,473			360	18,08	– 0,047	1,25	– 3,4	3,6	– 1,9	– 0,05
20G	MH	27	0,378			0	30,1	– 1,09	0,918	– 0.692	0,229	– 0,028	
AH13	OSD	230	0,513		354,9			32,2	2,11	– 1,55	0,506	– 0,061	
13D	OSD	26	0,281		452,3			$5{,}79\cdot10^3$	– 74,5	38,3	– 6,91		
13H	OSD	21	0,047		430,5			66,8	$-14{,}6\cdot10^3$	$14{,}6\cdot10^3$	$-7{,}2\cdot10^3$	$1{,}8\cdot10^3$	$-0{,}17\cdot10^3$
									– 128,7	64,2	– 11,1		

* AH7 - all heats in condition 7; AH7, 7G, 7M - [9]; AH23, 23A - [10]; 41 - B - [11];
AH5, 5B, 5M - [12]; AH20, 20G - [13]; AH13, 13D, 13H - [14]

quickly; therefore, of practical importance is mainly the range of β_e values from 0,6…0,8 to 2,2…2,3.

Stress rupture data for a large number of creep-rupture diagrams were extrapolated for one log-time cycle. It was established that in the case of the validity of the condition

$$\beta - 0{,}3 \div 0{,}4 < \beta_e < \beta + 0{,}3 \div 0{,}4, \qquad (12)$$

the following condition will also hold true for the MBD predictions:

$$S_2 \leq 0{,}1 \ldots 0{,}12. \qquad (13)$$

The results of processing the same stress rupture data [9 - 14] are given in Table 3. (LM, MH, and OSD parameters) and Table 4. (BDM-2). The values of S_1 in Tables 3. and 4. are close. We may suppose that the use of such a large number of redundant constants raises serious obstacles in the way of efficient development of prediction methods.

RESULTS AND DISCUSSION

As an example, Table 1. lists the results of processing the data [13] used as endpoints of 32 portions of SR diagrams for one heat. For all 283 portions of the curves for nine heats it was found that at $\sigma_{\alpha t} \leq 340$ MPa $\beta = \beta_3 =$ 1,4, at 340 MPa $< \sigma_{\alpha t} <$ 480 MPa $\beta = \beta_2 = 1{,}0$, and at $\sigma_{\alpha t}$ > 480 MPa $\beta = \beta_1 = 0{,}3$ (Table 2.). These values of β are used in Eq. (8). The values of S_1 and S_2 were calculated for all nine heats taken together, i.e., for 283 portions, and for each of nine heats separately (Figure 3., Table 2.). The calculations were performed similarly to those in [9 - 14]

Table 4. **Results of processing data [9 - 14] by BDM-2**
Tablica 4. **Rezultati obrade podataka [9 - 14] s BDM-2**

Heat	n	S_1	S_2	β_1	β_2	β_3
AH7*	370	0,335	0,099	1,1	1,0	0,8
7G	30	0,123	0,027	0,9	0,9	0,7
7M	46	0,159	0,051	1,1	1,0	0,7
AH23	182	0,144	0,039	0,96	1,02	1,06
23A	65	0,061	0,021	1,0	1,1	1,1
AH41	148	0,406	0,208	0,94	1,08	1,16
41B	24	0,335	0,196	1,0	1,4	1,2
AH5	459	0,206	0,099	1,1	1,2	0,9
5B	46	0,132	0,056	1,1	1,1	1,0
5M	60	0,153	0,075	1,12	1,16	1,0
AH20	283	0,459	0,156	1,4	1,1	0,3
20G	32	0,229	0,102	1,34	0,74	0,14
AH13	267	0,433	0,166	1,1	1,0	0,6
13D	23	0,122	0,046	1,0	0,4	0,4
13H	26	0,132	0,032	1,0	0,8	0,6

AH7 - all heats in condition 7.

by the parametric methods [1 - 3]. The calculation results are given in Tables 2. - 4.

As follows from Table 2., the Manson-Haferd parametric method gives better prediction results. However, it should be taken into account that in all the cases, the BDM (Basic Diagram Method) data processing was carried out using at most three values of β_i, which is a physically justified quantity, since it can be recalculated into the constant n in the $t_r \sim \sigma^n$ relation.

Besides, as follows from Table 1., the predictions were often performed for two three or more log cycles of time and more. In the analysis using the parametric methods the focus is on one or two constants, while the description of the parametric curves often requires five or six empirical constants to which no meaning can be assigned (Table 3.).

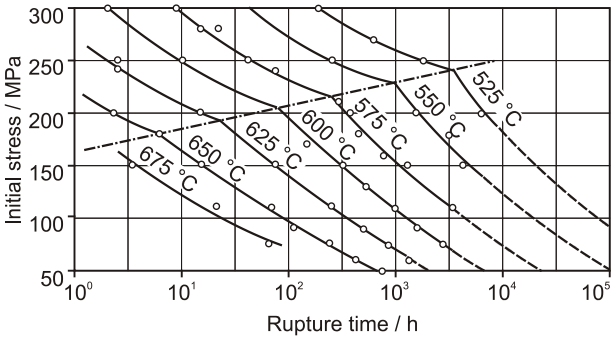

Figure 4. **Examples of instabilities for 2,25Cr-1Mo steel that lie along an oblique line in the stress-time plane on data [15]**
Slika 4. **Primjeri strukturne nestabilnosti za čelik 2,25Cr-1Mo u području točaka određenih kosom crtom (naprezanje - vrijeme) [15]**

Table 5. **Results of processing data [15] by the BDM-2**
Tablica 5. **Rezultati obrade podataka [15] s BDM-2**

No.	$\sigma_{\alpha t}$ / MPa	σ_{te} / MPa	αt / h	*te* / h	$\lg(\frac{te}{\alpha t})$	Δ_1	Δ_2	β_3	β_i
1	300	240	180	3300	1,263	0,64	– 0,23	0,68	
2	300	230	42	1000	1,377	0,62	– 0,23	0,75	
3	300	217	9	250	1,444	0,51	– 0,19	0,87	
4	300	206	1	77	1,631	0,51	– 0,19	0,92	
5	300	200	180	6700	1,571	0,49	– 0,20	0,93	
6	300	150	42	4700	2,049	0,31	– 0,15	1,13	
7	300	100	9	4400	2,689	0,18	– 0,11	1,23	1,3
8	300	75	1,8	2900	3,207	0,20	– 0,14	1,24	
9	300	100	180	80000	2,648	0,23	– 0,14	1,22	
10	300	50	42	1000	3,377	0,06	– 0,06	1,29	
11	300	50	9	21000	3,368	0,02	0,01	1,30	
12	300	50	1,8	6200	3,537	0,07	– 0,06	1,28	
13	250	193	1,8	23	1,106	0,35	– 0,13	0,91	
14	250	50	1,8	1800	3,000	0,11	0,10	1,34	
15	200	180	2,3	7	0,483	0,24	– 0,11	0,82	
16	240	200	3300	6700	0,308	0,07	0,04	1,95	
17	230	150	1000	4700	0,672	0,15	0,09	1,91	
18	217	100	250	4400	1,246	0,07	0,05	1,68	
19	206	75	77	2900	1,576	0,02	0,01	1,61	
20	196	50	23	1800	1,894	0,04	0,04	1,62	
21	180	50	7	800	2,058	0,21	– 0,24	1,47	1,6
22	157	75	3	80	1,426	0,18	– 0,13	1,43	
23	240	100	3300	80000	1,385	0,08	0,06	1,68	
24	230	50	1000	100000	2,000	0,08	0,10	1,65	
25	217	50	250	21000	1,924	0,09	0,11	1,66	
26	206	50	77	6200	1,906	0,06	0,07	1,64	
$S_1 = 0{,}291$; $S_2 = 0{,}135$									

The results of processing the data [13] by the Manson-Haferd method and BDM are presented in Table 2. As is seen, the S_1 values obtained by the BDM are generally lower than those obtained by the Manson-Haferd method. It should be noted that such a limited amount of data processed cannot be sufficiently representative for a general conclusion. The BDM calculations yielded higher S_1 values in 70 % of cases. Analyzing these data, one should pay attention to an important circumstance. If the S_1 values obtained by the parametric methods were comparatively low, increasing the number of constants caused a reduction in the S_1 values. At higher S_1 values, i.e., in the case of more complicated predictions, the increase in the number of constants did not result in decreasing the S_1 values.

In the data processing by the Manson-Haferd method, the number of the constants used for each of nine heats was 7, 6, 7, 7, 6, 7, 6, 6, and 7. The general parametric curve was calculated for $T_a = 340$, $\lg t_a = 18{,}0$, $b_0 = -0{,}48$, ..., i.e., with the use of seven such constants, which resulted in $S_1 = 0{,}473$. BDM calculations with the use of three β_i values, viz., $\beta_1 = 0{,}3$, $\beta_2 = 1{,}1$, and $\beta_3 = 1{,}4$, resulted in $S_2 = 0{,}459$. At $\beta_3 = 1{,}4$ common for all nine heats, the value of β_3 for each heat taken separately was 1,37; 1,40; 1,40; 1,55; 1,42; 1,34; 1,48; 1,43 and

1,32; the values of T_a and lg t_a for each heat were 0, 610, 0, 0, 0, 0, 0, 600 and 29,6; 31,8; 10,2; 27,5; 31,1; 30,1; 28,2; 30,4; 10,2, respectively.

It should be emphasized that the parametric methods and the BDM differ considerably. When the parametric methods are used, the main task consists in correlating experimental data by plotting an averaged parametric curve, whereas for the BDM the averaging is performed using the β_i values. In addition, detailed data on each portion of stress-rupture diagrams are obtained in the form $\beta_i - \beta_e$ (Figure 3.).

Studies [15, 16] lead to the conclusion that the development of more general prediction methods is called for by the necessity to solve more complicated prediction problems. Typical examples of such problems can be found in [15], in particular the data in Figure 4. According to [15, 16], spline functions should be used instead of Eq. (4) in such complex cases to enhance the flexibility of the shape of SR curves. In the given case, the curves (Figure 4.) should be divided into separate pieces joined at the endpoints. One shape of the relation should be applied to values above the endpoints and another to those below them Above a spline point, one form of the dependence should be used; below it, the other, namely, for the stresses above the endpoints, the relation may be $G = A + B \lg \sigma + C/\sigma$ and for those below them $G = A' + B' \lg \sigma + C' \sigma$.

Now consider the performance of the BDM, which can be judged from the results of the corresponding data analysis given in Figure 4. and Table 5.

Table 5. presents the results of an ordinary processing by the BDM-2. The value of $S_2 = 0{,}135$ can be accepted as reasonable if we take into account that the predictions were made with the use of only two constants $\beta_2 = 1{,}3$ and $\beta_3 = 1{,}6$. Finally, it should be emphasized that out of 26 estimates, 14 were made for 1,5 log cycles and more, including 8 estimates for two log cycles and more, and 4 estimates for three log cycles and more.

CONCLUSIONS

The structure of complex alloys deformed at elevated temperatures is determined by a complicated function of a large number of interrelated variables. Considering the above conditions, the investigations performed make it possible to draw the following conclusion. The generalization and systematization of the known experimental data with a careful consideration of the general and specific features of the material behavior can lead to novel, more efficient methods for predicting the long-term strength of heat-resistant steels and alloys.

REFERENCES

[1] F. R. Larson, J. Miller: Time - temperature relationship for rupture and creep stresses, Trans. ASME. 74 (1952) 5, 765 - 775.

[2] S. S. Manson, A. M. Haferd: A linear time - temperature relation for extrapolation of creep and stress rupture data, NASA TN 2890., 1953.

[3] R. L. Orr, O. D. Sherby, J. E. Dorn: Correlation of rupture data for metals at elevated temperatures, Trans. ASM. 46 (1954), 113 - 128.

[4] V. V. Krivenyuk: Prediction of Long-Term Strength of Refractory Metals and Alloys [in Russian], Nauk. Dumka, Kiev (1990), 248.

[5] J. B. Conway, P. N. Flagella: Creep-rupture data for refractory metals to high temperatures, New York-London-Paris: Gordon and Breach Science Publisher, 1971, p. 787.

[6] Creep strength in steel and high-temperature alloys, Proc. of the Iron and Steel Institute, University of Sheffield, 1972, p. 273.

[7] G. S. Pisarenko, V. V. Krivenyuk: New approach to the prediction of long-term strength of metals, Dokl. AN SSSR, Mekhanika 312 (1990) 3, 558 - 562.

[8] V. V. Krivenuyk: Long-term creep-rupture prediction for metallic materials, Probl. Prochn. (2003) 4, 403 - 412.

[9] Data sheets on the elevated-temperature properties of 0,2C Steel, NRIM. Tokyo (1992) 7B, 24.

[10] Data sheets on the elevated-temperature properties of 20Cr-20Ni-20Co-4W-4Mo-4(Nb+Ta) superalloy, Ibid. Tokyo (1989) 23B, 28.

[11] Data sheets on the elevated-temperature properties of nickel based 15,5Cr-8Fe, Ibid. Tokyo (1999) 41A, 38.

[12] Data sheets on the elevated-temperature properties of 18Cr-10Ni-Ti stainless steel, Ibid. Tokyo (1987) 5B, 32.

[13] Data sheets on the elevated-temperature properties of 0,5Cr-0,5Mo steel, Ibid. Tokyo (1994) 20B, 28.

[14] Data sheets on the elevated-temperature properties of 12Cr Steel, Ibid. Tokyo (1994) 13B, 44.

[15] S. S. Manson, C. R. Ensign: A quarter-century of progress in the development of correlation and extrapolation methods for creep rupture data, J. of Engineering Materials and Technology 101 (1979), 317 - 325.

[16] R. M. Goldhoff: Towards the standardization of time - temperature parameter usage in elevated temperature data analysis, J. of Testing and Evaluation, JTEVA 2 (1974) 5, 387 - 424.